Fabrication of a Flexible Amperometric Glucose Sensor Using Additive Processes

Xiaosong Du,[a] Christopher J. Durgan,[a] David J. Matthews,[b] Joshua R. Motley,[a] Xuebin Tan,[b] Kovit Pholsena,[a] Líney Árnadóttir,[a,*] Jessica R. Castle,[c] Peter G. Jacobs,[c,d] Robert S. Cargill,[c] W. Kenneth Ward,[c,z] John F. Conley Jr.,[b,z] and Gregory S. Herman[a,z]

[a]*School of Chemical, Biological, and Environmental Engineering, Oregon State University, Corvallis, Oregon 97331, USA*
[b]*School of Electrical Engineering and Computer Science, Oregon State University, Corvallis, Oregon 97331, USA*
[c]*Pacific Diabetes Technologies, Portland, Oregon 97201, USA*
[d]*Oregon Health & Science University, Portland, Oregon 97239, USA*

This study details the use of printing and other additive processes to fabricate a novel amperometric glucose sensor. The sensor was fabricated using a Au coated 12.7 μm thick polyimide substrate as a starting material, where micro-contact printing, electrochemical plating, chloridization, electrohydrodynamic jet (e-jet) printing, and spin coating were used to pattern, deposit, chloridize, print, and coat functional materials, respectively. We have found that e-jet printing was effective for the deposition and patterning of glucose oxidase inks with lateral feature sizes between $\sim$5 to 1000 μm in width, and that the glucose oxidase was still active after printing. The thickness of the permselective layer was optimized to obtain a linear response for glucose concentrations up to 32 mM and no response to acetaminophen, a common interfering compound, was observed. The use of such thin polyimide substrates allow wrapping of the sensors around catheters with high radius of curvature $\sim$250 μm, where additive and microfabrication methods may allow significant cost reductions.

Advances in accurate sensing of blood glucose concentrations have contributed to improved control of blood sugar levels for patients with type 1 diabetes.[1,2] Type 1 diabetes is a pancreatic and endocrine disease in which blood glucose is poorly controlled because the patient's beta cells cannot generate sufficient insulin. Long-term exposure to elevated glucose levels can lead to complications such as retinopathy, neuropathy, nephropathy, and cardiac disease. There is no known cure for type 1 diabetes and it has traditionally been controlled by the use of frequent glucose measurement with a blood glucose meter and insulin injections in order to maintain blood glucose levels within an acceptable range. The recent development of continuous glucose sensors now allows real-time monitoring of blood sugar levels.[2] Portable infusion pumps allow continuous subcutaneous infusion of insulin and deliver basal and bolus doses of insulin to assist in maintaining glycemic control.[3,4]

A glucose sensor is a critical component of an artificial pancreas and research in this area has been extensive.[1,2] An artificial pancreas integrates continuous glucose sensing with automated delivery of the hormone insulin with or without glucagon to appropriately control glucose levels.[5–8] The concept of a closed loop artificial pancreas has been around for many years, beginning with the work of Albisser et al.[9,10] The number of research studies on artificial pancreas controllers has increased in recent years including those using model predictive controllers,[11–13] those using proportional integrative derivative (PID) or PID-like controllers,[14–18] and those using fuzzy logic.[19,20]

A sensor within an artificial pancreas needs to accurately measure glucose concentrations over the wide range typically found in patients with diabetes (i.e. 2–30 mM in the interstitial fluid) to minimize the risk of over/under delivery of insulin and glucagon.[1,2] Other desirable characteristics of a sensor for an artificial pancreas are long working lifetimes to minimize the inconvenience of replacing the device, and low cost to facilitate widespread usage. Amperometric glucose sensors are specified to work for 7 days, and typically have a mean absolute relative difference (MARD, percent error) in the 12–18% range. Castle et al. found that redundancy of sensing elements can somewhat reduce

the MARD and can markedly reduce the frequency of very large egregious errors.[21]

Continuous glucose sensors have been made using a wide variety of substrates and electrode materials. Harrison et al.[22] fabricated a glucose sensor based on a platinum wire, which was dip-coated with an active enzyme layer. Yu et al.[23] designed a coiled platinum wire with an integrated Ag/AgCl reference electrode wire, which was successfully tested in rats for a period of up to 56 days. Endo et al.[24] developed another sensor with integrated Ag/AgCl reference electrode and a platinum wire which provided continuous glucose monitoring in anesthetized animals. Other glucose sensor devices have been fabricated on flexible polymer substrates. Kudo et al.[25] constructed a sensor on a polydimethylsiloxane (PDMS) substrate, with platinum working electrode and Ag/AgCl counter/reference electrode. Sensors with the same design were also fixed to PDMS contact lenses and successfully tested in rabbits.[26] Li et al.[27] used a polyimide substrate to fabricate a spirally rolled flow-through catheter for implantation in blood vessels, where the sensor had gold working and counter electrodes with a Ag/AgCl reference electrode.

Additive manufacturing is of increasing interest for the fabrication of high value components, which can be customizable with reduced environmental impact.[28] Key benefits of additive manufacturing are (i) the reduction of processing steps compared to standard microfabrication based approaches, which require multiple deposition, pattern, and etch steps for each functional layer, (ii) the potential reductions in cost that result from reduced steps, and (iii) unique functionality including integration on flexible substrates.[29] Recently additive manufacturing has become of much more interest for medical applications, where unique two- and three-dimensional structures can be effectively constructed for individual patients.[30,31] Printing is one of the most appealing additive manufacturing approaches since it is inherently low cost, and can simultaneously deposit and pattern the films. Examples of inkjet printed materials include glucose oxidase,[32,33] metal conductors,[34] and adhesives.[35]

In this paper, we demonstrate the advantage of printing and additive processes to fabricate amperometric glucose sensors using a thin, metallized, and flexible polyimide substrate as a starting material. High-resolution electrohydrodynamic (e-jet) printing was used to pattern functional glucose oxidase (GOx) enzyme inks on plated platinum working electrodes. Amperometric measurements indicate

*Electrochemical Society Active Member.
[z]E-mail: kward@pacificdt.com; john.conley@oregonstate.edu; greg.herman@oregonstate.edu

that the enzyme is still active after e-jet printing. The thickness of the permselective layer was optimized to selectively limit the glucose diffusion rate through the membrane compared to oxygen diffusion, which allows for a linear response to the glucose concentration over the range of interest. Our results illustrate that low cost additive manufacturing approaches can be used to fabricate amperometric glucose sensors, and these can potentially be applied to other enzymatic sensing approaches.

Experimental

Materials.— Bovine serum albumin (BSA), 1H,1H,2H,2H-perfluorodecanethiol, ferric nitrate, acetaminophen and octadecanethiol were purchased from Sigma Aldrich (St. Louis, MO). Thiourea and glucose was obtained from Alfa Aesar (Ward Hill, MA). Glutaraldehyde was acquired from Electron Microscopy Sciences (Hatfield, PA). Glucose oxidase and $FeCl_3$ were obtained from Amresco (Solon, OH). NaCl, KCl, NaH_2PO_4, Na_2HPO_4 were acquired from Avantor Performance Materials (Center Valley, PA). The e-jet printing needle (glass micropipette) was purchased from World Precision Instruments (Sarasota, FL). Perfluorosulfonic acid (PFSA) in 1-propanol and water was purchased from Ion Power (New Castle, DE). The photoresist SU-8 was acquired from Microchem (Westborough, MA). Sylgard 184 PDMS was obtained from Dow Corning (Midland, MI). The Pt and Ag plating solution were purchased from Technic (Cranston, RI). Au (150 nm thick) on 12.7 μm polyimide (PI) film was acquired from Sheldahl (Northfield, MN). Milli-Q water (18.2 MΩ cm) was used in all sample preparation.

Amperometric sensor electrode fabrication.— A glucose sensing device comprised of six Pt working electrodes and one common Ag/AgCl reference/counter electrode, was patterned on a Au coated PI substrate by micro-contact printing as has been described previously.[36–38] In brief, a PDMS stamp was fabricated from an SU-8 master that was patterned on a silicon substrate using photolithography (MJB3, Suss MicroTec Group, Garching, Germany). A self-assembled monolayer (SAM), octadecanethiol, was applied to the PDMS stamp by immersion in 2 mM octadecanethiol (ethanol as solvent) for 5 min. The SAM was transferred from the PDMS stamp to the Au film on the PI susbtrate after ~15 s contact time. After the SAM was transferred the unprotected Au was etched at a rate of 10 nm/min in 20 mM Fe$(NO_3)_3$ and 30 mM thiourea solution at pH ~ 2.[39] The octadecanethiol SAM was removed from the Au surface by UV-Ozone treatment followed by an ethanol rinse. The surface was subsequently cleaned by an oxygen plasma (PE-100, Plasma Etch, Inc. Carson City, NV).

Selective electroplating was performed by making electrical contact to the working or reference electrode contact pads. Pt (~12 nm) was electroplated on the working electrodes at a plating bath temperature of 65°C and a current density ~54 A/m² for 40s. Ag (~200 nm) was electroplated on the counter/reference electrode at a plating bath temperature of 30°C and a current density ~107 A/m² for 25s. Chloridization of the Ag was performed by reacting the Ag electrode with a 50 mM $FeCl_3$ solution for 2 min at room temperature.[40] The chloridization was performed soon after electroplating to minimize the formation of silver oxide and silver sulfide. Electroplated Ag showed homogeneous coverage on Au coated PI substrates, where a uniform layer of sub-micron AgCl particles was observed after chloridization.

A custom-built e-jet printer was used to deposit and pattern GOx ink onto the Pt working electrodes. The e-jet printer features a high-voltage amplifier (Trek 677B, Trek, Inc. Medina, NY), which applies a voltage between the printing needle and the substrate. The substrate was placed on a carrier that has a computer controlled motorized stage using x and y-axis linear steppers (Parker MX80L T03MP, Parker Hannifin Corp. Cleveland, OH) to move the substrate with respect to the printing needle, and a two-axis tilting stage (Edmund Optics 70 mm metric Micrometer Tilt Stage, Edmund Optics Ltd. York, UK) to level the substrate. The printing needle can be moved up and down using a computer controlled z-axis linear stepper motor (Parker MX80ST

02MSJ, Parker Hannifin Corp. Cleveland, OH). The printing process was observed through a microscope camera (Edmund Optics Infinity2, Edmund Optics Ltd. York, UK) that was illuminated with fiber optic lamps. Custom control software was written in LabView to control the stage x-y motion and velocity, and the pulse voltage, duration, and frequency. The printing needle was coated with a film of 20 nm sputtered 60/40 Au/Pd alloy to provide electrical conductivity, using a Cressington Sputter Coater 108auto. Needles with an inner diameter tip of 5 and 30 μm were used for these studies. Prior to printing, the needle tip was dipped in liquid 1H,1H,2H,2H-perfluorodecanethiol for one minute, which forms a hydrophobic SAM on the outer metal surface of the needle. This monolayer prevents excessive wetting of the needle by the GOx ink. Printing backpressure was controlled by a pressure transducer (ControlAir 500-AF, ControlAir Inc. Amherst, NH) that was connected to a syringe and forced the ink to the tip of the needle. Normal operating pressures were between 0.5 and 3 psi. The needle bias was set using a National Instruments controller (SCB-80, National Instruments Inc. Austin, TX) and a voltage amplifier, which was connected to the printing needle, while the substrate was grounded. Printing was achieved by pulsing the voltage in a square wave, where the frequency and amplitude of the wave were controlled by the software. To print in the controlled cone-jet mode, the lower voltage of the pulse was sufficient to hold the fluid meniscus in a Taylor cone whereas the higher voltage of the pulse caused fluid to eject from the tip of the cone.[41–43] To print specific patterns, the e-jet printing software reads a text file which contains commands to move the x- and y- stages, and to modulate the voltage. Adjusting the stage velocity and voltage pulsing frequency allows the control of droplet size and spacing between droplets. Prior to printing the substrate was treated with UV/ozone for 15 min to ensure good surface wetting. The printed patterns were characterized using atomic force microscopy (AFM, Bruker Innova, Santa Barbara, CA), optical microscopy (Zeiss Axiotron, Pleasanton, CA), and optical profilometry (ZeScope, Zemetrics, Zygo Corp. Middlefield, CT).

Printing parameters on the e-jet printer (voltage, pulse frequency, stage velocity, pressure, and working distance) were adjusted to give repeatable patterning. Printing was accomplished by biasing the needle at a constant 600 V, which was pulsed with a peak of up to 800 V for frequencies between 10–30 Hz. The distance between the printing needle and the substrate was typically 100 microns. The printed GOx patterns were characterized by optical microscopy and AFM to help optimize the printing parameters for uniform coverage of the electrode surfaces. To improve wetting of the GOx ink we performed a UV/ozone treatment of the Pt/Au/PI substrates prior to printing.

Glucose oxidase ink.— An aqueous GOx and BSA ink was developed for e-jet printing of the enzyme films. The dissolved GOx was stabilized with the addition of 5% v/v of glycerol to the aqueous base. The glycerol helps to keep the enzyme from crystallizing prematurely, and reduces the surface tension of the GOx ink, which aids in printing. It was determined that a mixture of 18 mg GOx and 2 mg BSA per mL of water gave good mechanical stability of the printed enzyme layer, and provided good sensitivity to glucose. In order to crosslink the GOx film onto the sensor, the GOx and BSA were premixed with 0.4 mg/mL glutaraldehyde just prior to printing on the Pt working electrode surface. The total GOx and BSA concentration was 20 mg/mL, which gave a thick cross-linked enzyme layer, while still allowing uniform printing for over 40 minutes (i.e., the time required to print several devices). The functional ink conductivity, viscosity, and surface tension were determined to be 3.2×10^5 μS/m, 1.1×10^{-3} Pa · s, and 60 mN · m^{-1}, respectively.

Permselective membrane.— Solutions between 1% and 30% by weight of PFSA in 1-propanol and water were used to fabricate thin polymer films onto the surfaces by spin-coating (Laurell WS-400BZ-6NPP/LITE, Laurell Technologies Corp. North Wales, PA). Polymer films were formed using rotation speeds of 1000–3000 RPM for

60–90 seconds, and the film thicknesses were measured by profilometry (Alpha Step 500, KLA-Tencor Inc. Milpitas, CA).

Electrochemical glucose sensing.— Characterization of glucose sensor devices was performed by placing the sensor in an electrochemical cell containing phosphate buffered saline (PBS) solution composed of 137 mM NaCl, 2.5 mM KCl, 4 mM NaH_2PO_4, and 16 mM Na_2HPO_4, with a pH of 7.4. The electrochemical cell solution was purged with Ar during experiments, in order to stir the solution and reduce oxygen levels in the solution to that of mammalian interstitial fluid (45 torr or 0.08 mM).[44] Amperometric measurements were obtained with a BioLogic SP-200 Potentiostat (BioLogic, Knoxville, TN). Oxygen concentrations were measured with a NeuLog NEU-205 oxygen sensor (NeuLog Inc. Rishon-Lezion, Israel). During amperometric measurements the Pt working electrodes were polarized at +600 mV relative to the integrated Ag/AgCl reference electrode, and the current was monitored while the concentration of glucose was increased by pipetting in concentrated glucose solutions. The glucose concentration was varied between 0–32 mM for these measurements, which corresponds to the relevant clinical interstitial fluid glucose levels of diabetic patients. All the experiments were performed on 3 separate devices.

Results and Discussion

Sensor design.— In Figure 1a we show the wrapping of the sensors around catheters with high radius of curvature ∼250 µm. A cross

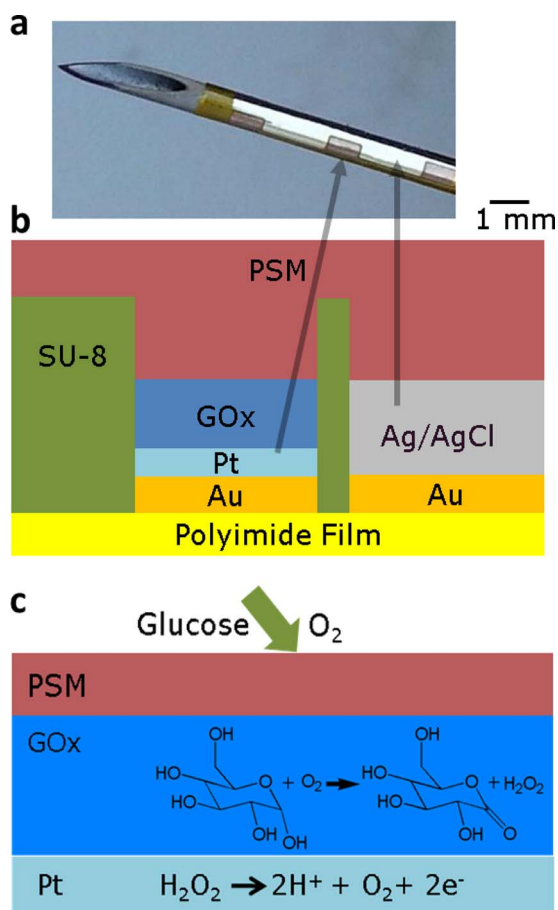**Figure 1.** (a) The wrapping of the sensors around catheters with high radius of curvature ∼250 µm, (b) schematic of a cross section of the amperometric glucose sensor on polyimide substrate and (c) schematic of the senors function and chemical reactions in the glucose oxidase (GOx) layer and on Pt working electrodes.
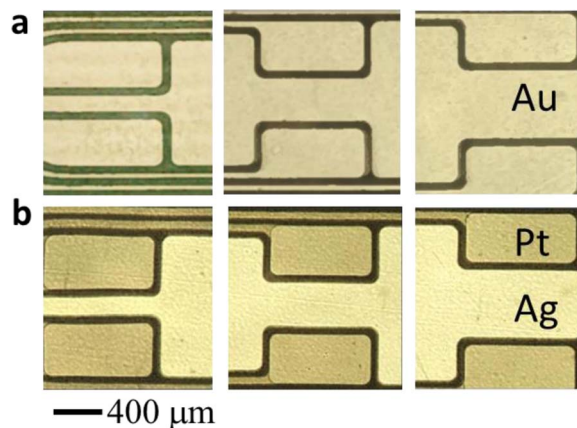

Figure 2. Optical microscopy images of (a) patterned Au on PI substrate prepared via microcontact printing, and (b) after Pt and Ag electrodes deposition by electroplating.

sectional schematic of the sensor with each of the layers labeled (not to scale) has been shown in Figure 1b. The three key factors that allow accurate glucose sensing are formation of platinum electrodes with well-defined areas and good catalytic activity, deposition of glucose oxidase layers with uniform thickness, and use of permselective layers with good control over the relative effective diffusion rates of glucose and oxygen. Each of these processes will be discussed below. In Figure 1c we show the operating principle of an amperometric glucose sensor. In brief, the oxidation of glucose by molecular oxygen is catalyzed by immobilized GOx, which results in the formation of H_2O_2. The H_2O_2 is then oxidized at the Pt working electrode that is biased at +600 mV with respect to the Ag/AgCl reference electrode, resulting in an electrochemical current.[1] This electrochemical current can be used to quantify the amount of glucose in the interstitial fluid.

In Figure 2a we show optical microscope images of Au films on PI substrates. The Au films were patterned using microcontact printing and etching. These patterns replicated the stamp without visible defects or loss of resolution. The yield of these Au microelectrodes exceeded 90% on a typical batch of devices, as determined by optical microscopy and two-point electrical measurements. For electroplating, we used a patterned photoresist to define the regions where the Pt and Ag were electroplated on the Au microelectrodes. Electroplating of either Pt or Ag layers was conducted by placing the substrate in the appropriate plating solution and applying a potential to achieve the desired current density. The thickness of plated Ag (200 nm) and Pt (12 nm) film was determined by profilometry. The plated Ag counter/reference electrode and Pt working electrodes are shown in Figure 2b. Each working electrode has a planar surface area of approximately 0.32 mm^2, whereas the total reference electrode area was approximately 4.74 mm^2. A 2 µm thick SU-8 layer was used as a passivation layer on the sensor and to provide wells for the working or counter/reference electrodes.

Electrohydrodynamic printing.— In Figure 3 we show uniformly spaced e-jet printed droplets of very small GOx features (∼5 µm in diameter) which were obtained using a needle with an inner tip diameter of 5 µm. These results indicate that very fine and uniform GOx features can be obtained using e-jet printing compared to ∼15–40 µm diameter dots produced by typical inkjet printing.[45] Further optimization of the printing parameters of e-jet printed GOx inks was necessary to pattern uniform films. For these studies different drop spacings were obtained by adjusting the stage velocity (v) and voltage square wave pulse frequency (f), while using a needle with an inner tip diameter of 30 µm. Using a stage velocity of 1200 µm/s and a frequency of 10 Hz (Figure 4a), we found that the ratio of drop generation and the voltage frequency was ∼ 1. This ratio can be maintained up to f = 20 Hz (Figure 4b), however above f = 30 Hz the printed

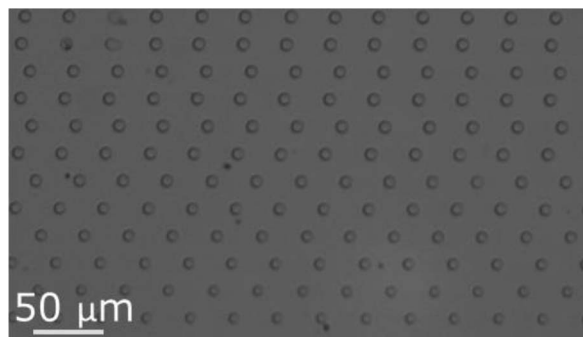**Figure 3.** High-resolution e-jet printing of GOx dot array using a 5 μm diameter nozzle at f = 20 Hz, v = 700 μm/s.

Figure 5. (a) E-jet printing of enzyme ink on Pt working electrodes of glucose sensor and (b) optical profilometry images of 400×800 μm^2 (working electrode size) pad printed twice over the same area at f = 20 Hz, v = 500 μm/s.

drops (Figure 4c) showed irregular size and/or spacing. This may be due to Taylor cone distortion, with poor recovery at higher frequencies resulting in a reduction in the ratio of drop generation and voltage frequency to below 1.[41] Therefore, the optimized pulse frequency to print our GOx ink was determined to be 20 Hz, which allowed us to generate the most uniform drop patterns for high-speed printing. The stage velocity was also optimized to go from isolated droplets to continuous lines of GOx ink, by slightly overlapping each droplet with its previous neighbor. At a frequency of 20 Hz and velocity of 1200 μm/s (Figure 4d), multiple small droplets can be distinguished, which results from the stage velocity being too high. At a frequency of 20 Hz with the stage velocity reduced to 700 μm/s (Figure 4e), the profile of individual droplets could still be recognized within the coalescing line. When the stage velocity was reduced further to 500 μm/s (Figure 4f), we were able to produce a smooth, continuous line with no evidence of individual droplets. We show AFM measurements in Figure 4g to 4h, for the same printing conditions as Figure 4d to 4f, respectively. These AFM images confirm that individual drops, elongated drops, and continuous lines were observed, respectively. The line width was determined to be approximately 30 μm wide for the printing conditions optimized for continuous lines.

Once continuous lines were obtained, a printing pattern with line spacing of 30 μm was used so that adjacent lines could coalesce and create a continuous film of GOx on the Pt working electrodes. In Figure 5a we show images of the e-jet printer depositing the GOx ink on two working electrodes of the sensor. It takes approximately 1 min to print two layers of GOx on a single working electrode, which corresponds to a total printing time of 6 min for the entire amperometric
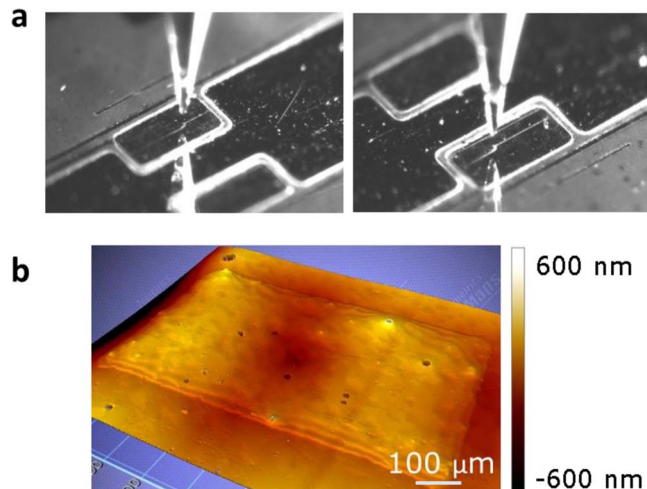
sensor. An optical profilometry image of a single working electrode with two layers of e-jet printed GOx is shown in Figure 5b.

Electrochemical test.— Spin-coating was used to provide uniform film thicknesses for the permselective membrane (PSM), which allowed us to evaluate the effect of PSM film thickness on sensor performance.[46,47] It has been suggested that exposing the cross-linked GOx layer to concentrated acidic polymer solution may denature some of the enzyme.[22] Therefore, a thin "base coat" using 1% PFSA solution, about 60 nm thick, was applied before subsequent applications of thicker membranes with more concentrated PFSA solutions. Chronoamperometric data was obtained after application of the PSM on the flexible glucose sensors. The experimental data is shown in Figure 6a where the amperometric current is monitored for three different PSM thicknesses. In all cases the current increases in a stepwise fashion as the glucose concentration is increased. The increase in amperometric current is plotted versus glucose concentration in Figure 6b. In the upper portion of Figures 6a and 6b we show data from a two-coat membrane, with a total PFSA thickness of 300 nm. A highly nonlinear current response to glucose concentration was obtained, which suggests that the film does not effectively limit diffusion of glucose to the enzyme layer, and the oxidation rate of glucose is limited by low oxygen concentrations in the glucose solution (to approximate the O$_2$ concentration in the interstitial fluid). We found that increasing the PFSA membrane thickness to 3 μm significantly reduced the amperometric current (compared to the 300 nm PFSA membrane), but did not significantly extend the linear working range of the glucose sensor. The 3 μm PFSA coated sensor still only gave a linear response up to 15 mM of glucose. A nonlinear current response was observed above this concentration since glucose oxidation was again limited by oxygen concentrations through the membrane, which suggests that the 3 μm thick PSM still does not effectively limit diffusion of glucose to the enzyme layer. An even thicker 7 μm coating of PFSA further reduced the amperometric current, however it also improved the sensor function such that a linear sensor response up to 32 mM glucose (slope of current density vs. glucose concentration $\sim 4.8 \times 10^{-3}$ μA•(mm^2•mM)$^{-1}$) could be obtained. The extended linear region of this sensor is a result of an optimized membrane thickness that limits the flux of glucose with respect to oxygen through the membrane layer to the GOx enzyme layer, such that the enzyme reaction is limited by glucose rather than oxygen concentration.

Since PFSA is negatively charged, it has been shown to effectively limit the diffusion of negatively charged interfering compounds (e.g., ascorbic and uric acids).[48] However it is necessary that the PFSA
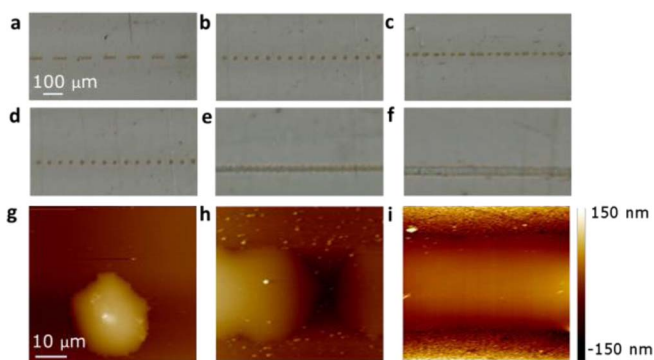

Figure 4. E-jet printed GOx with pre-mixed glutaraldehyde on Pt/Au/PI substrate. Optical images of printed dots at (a) f = 10 Hz, (b) f = 20 Hz, and (c) f = 30 Hz, printing speed is constant v = 1200 μm/s. Optical images of printed patterns at (d) v = 1200 μm/s, (e) v = 700 μm/s, and (f) v = 500 μm/s, pulse frequency is constant f = 20 Hz. AFM images (50×50 μm^2) of printed patterns at (g) v = 1200 μm/s, (h) v = 700 μm/s, and (i) v = 500 μm/s, pulse frequency is constant f = 20 Hz.
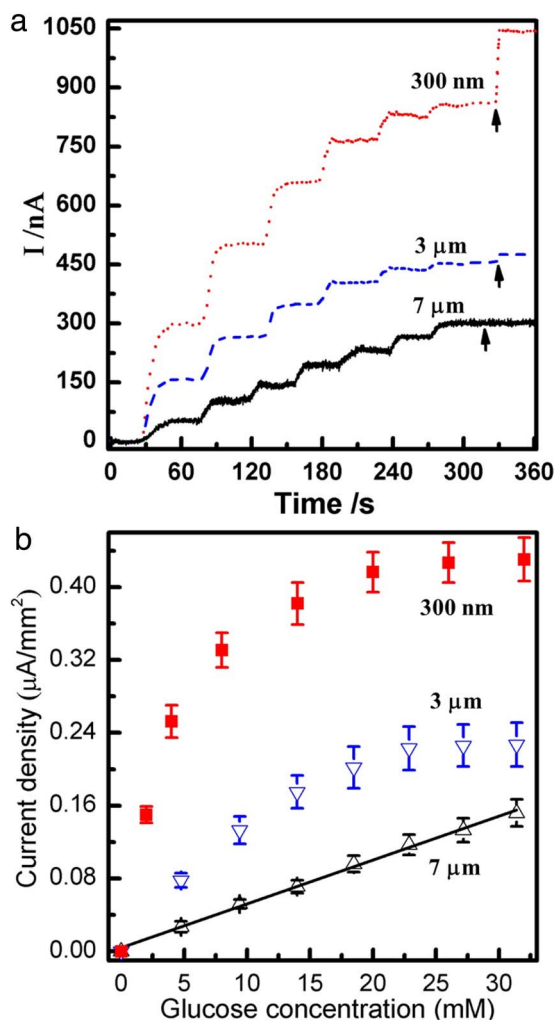
Figure 6. (a) Chronoamperometry of glucose sensor response to glucose concentration with printed GOx on Pt working electrodes and 300 nm, 3 μm and 7 μm thick outer PFSA membrane. Arrows indicate addition of 0.13 mM acetaminophen. (b) Current density vs. glucose concentration for these devices.

membrane also limits the diffusion of neutral interfering compounds such as acetaminophen, which can be oxidized directly on the Pt indicating electrodes.[49] Prior studies have shown that acetaminophen interference can be eliminated when PFSA is used as an inner membrane.[50,51] For our glucose sensor, PFSA was used as an outer membrane and it was necessary to determine if this structure can also block interference molecules. The arrows in Figure 6a indicate when 0.13 mM of acetaminophen was added to the electrolyte at the end of the experiment. A rapid increase in current was observed for the 300 nm PFSA membrane, indicating that acetaminophen readily diffuses through the thin membrane. For the 3 μm thick PFSA membrane there was only a slight current increase due to acetaminophen interference, indicating that acetaminophen still diffuses through this thicker membrane. However, we found that interference of acetaminophen was to-

tally suppressed when using the 7 μm thick PFSA membrane, which suggests that thicker PFSA membranes are effective in minimizing interference from acetaminophen. The glucose sensor response was also tested six months after fabrication and showed negligible signal loss (see Table I).

Conclusions

This study demonstrates that a continuous glucose sensor can be fabricated on a flexible polyimide substrate using additive technologies. We were able to use electrohydrodynamic printing to deposit and pattern a biological ink (containing glucose oxidase, bovine serum albumin, and glutaraldehyde as a cross-linking agent) with high resolution on the sensors working electrodes. The GOx enzyme was found to be active after e-jet printing. PFSA was used as a permselective membrane and its thickness was optimized to obtain a linear response for glucose concentrations up to 32 mM, as well as to minimize the detection of interfering molecules (e.g., acetaminophen). The flexible sensor design developed in these studies can ultimately be used within a closed loop artificial pancreas control system thereby reducing the number of components in such a system.

References

1. J. Wang, *Chemical Reviews*, **108**, 814 (2007).
2. S. P. Nichols, A. Koh, W. L. Storm, J. H. Shin, and M. H. Schoenfisch, *Chemical Reviews*, **113**, 2528 (2013).
3. C. D. Block, B. Manuel-y-Keenoy, and L. Van Gaal, *Journal of diabetes science and technology*, **2**, 718 (2008).
4. W. K. Ward, J. R. Castle, P. G. Jacobs, and R. S. Cargill, *Journal of diabetes science and technology*, **8**, 568 (2014).
5. C. M. Girardin, C. Huot, M. Gonthier, and E. Delvin, *Clinical biochemistry*, **42**, 136 (2009).
6. A. Heller and B. Feldman, *Chemical Reviews*, **108**, 2482 (2008).
7. H. Lee, B. A. Buckingham, D. M. Wilson, and B. W. Bequette, *Journal of diabetes science and technology*, **3**, 1082 (2009).
8. R. Mauseth, Y. Wang, E. Dassau, R. Kircher, D. Matheson, H. Zisser, L. Jovanovič, and F. J. Doyle, *Journal of diabetes science and technology*, **4**, 913 (2010).
9. A. M. Albisser, B. S. Leibel, T. G. Ewart, Z. Davidovac, C. K. Botz, and W. Zingg, *Diabetes*, **23**, 389 (1974).
10. A. M. Albisser, B. S. Leibel, T. G. Ewart, Z. Davidovac, C. K. Botz, W. Zingg, H. Schipper, and R. Gander, *Diabetes*, **23**, 397 (1974).
11. M. Breton, A. Farret, D. Bruttomesso, S. Anderson, L. Magni, S. Patek, C. Dalla Man, J. Place, S. Demartini, S. Del Favero, C. Toffanin, C. Hughes-Karvetski, E. Dassau, H. Zisser, F. J. Doyle, G. De Nicolao, A. Avogaro, C. Cobelli, E. Renard, and B. Kovatchev, Group o. b. o. T. I. A. P. S., *Diabetes*, **61**, 2230 (2012).
12. D. Bruttomesso, A. Farret, S. Costa, M. C. Marescotti, M. Vettore, A. Avogaro, A. Tiengo, C. Dalla Man, J. Place, A. Facchinetti, S. Guerra, L. Magni, G. De Nicolao, C. Cobelli, E. Renard, and A. Maran, *Journal of diabetes science and technology*, **3**, 1014 (2009).
13. B. Kovatchev, C. Cobelli, E. Renard, S. Anderson, M. Breton, S. Patek, W. Clarke, D. Bruttomesso, A. Maran, S. Costa, A. Avogaro, C. D. Man, A. Facchinetti, L. Magni, G. De Nicolao, J. Place, and A. Farret, *Journal of diabetes science and technology*, **4**, 1374 (2010).
14. G. M. Steil, K. Rebrin, R. Janowski, C. Darwin, and M. F. Saad, *Diabetes technology & therapeutics*, **5**, 953 (2003).
15. J. R. Castle, J. M. Engle, J. E. Youssef, R. G. Massoud, K. C. J. Yuen, R. Kagan, and W. K. Ward, *Diabetes Care*, **33**, 1282 (2010).
16. E. M. Watson, M. J. Chappell, F. Ducrozet, S. M. Poucher, and J. W. T. Yates, *Computer Methods and Programs in Biomedicine*, **102**, 119 (2011).
17. S. A. Weinzimer, G. M. Steil, K. L. Swan, J. Dziura, N. Kurtz, and W. V. Tamborlane, *Diabetes Care*, **31**, 934 (2008).
18. P. G. Jacobs, J. El Youssef, J. Castle, P. Bakhtiani, D. Branigan, M. Breen, D. Bauer, N. Preiser, G. Leonard, T. Stonex, and W. K. Ward, *Biomedical Engineering, IEEE Transactions on*, **61**, 2569 (2014).

Table I. Chronoamperometry of glucose sensor response to 32 mM glucose concentration with printed GOx on Pt working electrodes and a 300 nm, 3 μm, and 7 μm outer PFSA membrane. All the experiments were conducted 3 times.

PFSA coating	300 nm	3 μm	7 μm
As prepared	860 ± 40 (nA)	450 ± 40 (nA)	300 ± 30 (nA)
6 months storage	790 ± 40 (nA)	420 ± 30 (nA)	290 ± 30 (nA)

19. R. Mauseth, I. B. Hirsch, J. Bollyky, R. Kircher, D. Matheson, S. Sanda, and C. Greenbaum, *Diabetes technology & therapeutics*, **15**, 628 (2013).
20. E. Atlas, R. Nimri, S. Miller, E. A. Grunberg, and M. Phillip, *Diabetes Care*, **33**, 1072 (2010).
21. J. R. Castle, A. Pitts, K. Hanavan, R. Muhly, J. El Youssef, C. Hughes-Karvetski, B. Kovatchev, and W. K. Ward, *Diabetes Care*, **35**, 706 (2012).
22. D. J. Harrison, R. F. B. Turner, and H. P. Baltes, *Analytical Chemistry*, **60**, 2002 (1988).
23. B. Yu, N. Long, Y. Moussy, and F. Moussy, *Biosensors & bioelectronics*, **21**, 2275 (2006).
24. H. Endo, E. Takahashi, M. Murata, H. Ohnuki, H. Ren, W. Tsugawa, and K. Sode, *Fisheries Science*, **76**, 687 (2010).
25. H. Kudo, T. Sawada, E. Kazawa, H. Yoshida, Y. Iwasaki, and K. Mitsubayashi, *Biosensors & bioelectronics*, **22**, 558 (2006).
26. M. X. Chu, K. Miyajima, D. Takahashi, T. Arakawa, K. Sano, S. Sawada, H. Kudo, Y. Iwasaki, K. Akiyoshi, M. Mochizuki, and K. Mitsubayashi, *Talanta*, **83**, 960 (2011).
27. C. Li, J. Han, and C. H. Ahn, *Biosensors & bioelectronics*, **22**, 1988 (2007).
28. S. Mellor, L. Hao, and D. Zhang, *International Journal of Production Economics*, **149**, 194 (2014).
29. R. H. Reuss, D. G. Hopper, and J.-G. Park, *MRS Bulletin*, **31**, 447 (2006).
30. A. Cohen, R. Chen, U. Frodis, M. T. Wu, and C. Folk, *Rapid Prototyping Journal*, **16**, 209 (2010).
31. B. Vayre, F. Vignat, and F. Villeneuve, *Mechanics & Industry*, **13**, 89 (2012).
32. L. Setti, A. Fraleoni-Morgera, B. Ballarin, A. Filippini, D. Frascaro, and C. Piana, *Biosensors and Bioelectronics*, **20**, 2019 (2005).
33. C. C. Cook, T. Wang, and B. Derby, *Chemical Communications*, **46**, 5452 (2010).
34. J.-T. Wu, S. Lien-Chung Hsu, M.-H. Tsai, Y.-F. Liu, and W.-S. Hwang, *Journal of Materials Chemistry*, **22**, 15599 (2012).
35. A. Doraiswamy, R. Crombez, W. Shen, Y.-S. Lee, and R. J. Narayan, *The Journal of Adhesion*, **86**, 1 (2010).
36. J. C. Love, L. A. Estroff, J. K. Kriebel, R. G. Nuzzo, and G. M. Whitesides, *Chemical Reviews*, **105**, 1103 (2005).
37. D. Qin, Y. Xia, and G. M. Whitesides, *Nature protocols*, **5**, 491 (2010).
38. Y. Xia, E. Kim, X.-M. Zhao, J. A. Rogers, M. Prentiss, and G. M. Whitesides, *Science*, **273**, 347 (1996).
39. M. Geissler, H. Wolf, R. Stutz, E. Delamarche, U.-W. Grummt, B. Michel, and A. Bietsch, *Langmuir*, **19**, 6301 (2003).
40. B. J. Polk, A. Stelzenmuller, G. Mijares, W. MacCrehan, and M. Gaitan, *Sensors and Actuators B: Chemical*, **114**, 239 (2006).
41. M. W. Lee, D. K. Kang, N. Y. Kim, H. Y. Kim, S. C. James, and S. S. Yoon, *Journal of Aerosol Science*, **46**, 1 (2012).
42. J. U. Park, M. Hardy, S. J. Kang, K. Barton, K. Adair, D. K. Mukhopadhyay, C. Y. Lee, M. S. Strano, A. G. Alleyne, J. G. Georgiadis, P. M. Ferreira, and J. A. Rogers, *Nature materials*, **6**, 782 (2007).
43. J.-U. Park, J. H. Lee, U. Paik, Y. Lu, and J. A. Rogers, *Nano Letters*, **8**, 4210 (2008).
44. D. Wilson, W. F. Lee, S. Makonnen, S. Apreleva, and S. Vinogradov, in *Oxygen Transport to Tissue XXIX*, K. Kang, D. Harrison, and D. Bruley, Editors, p. 53, Springer US (2008).
45. L. Gonzalez-Macia, A. Morrin, M. R. Smyth, and A. J. Killard, *Analyst*, **135**, 845 (2010).
46. F. Moussy, D. J. Harrison, and R. V. Rajotte, *International Journal of Artificial Organs*, **17**, 88 (1994).
47. T. I. Valdes and F. Moussy, *Biosensors and Bioelectronics*, **14**, 579 (1999).
48. Y. Zhang, Y. Hu, G. S. Wilson, D. Moatti-Sirat, V. Poitout, and G. Reach, *Analytical Chemistry*, **66**, 1183 (1994).
49. W. K. Ward, M. D. Wood, and J. E. Troupe, *ASAIO Journal*, **46**, 540 (2000).
50. D. Moatti-Sirat, V. Poitout, V. Thomé, M. N. Gangnerau, Y. Zhang, Y. Hu, G. S. Wilson, F. Lemonnier, J. C. Klein, and G. Reach, *Diabetologia*, **37**, 610 (1994).
51. R. Vaidya, P. Atanasov, and E. Wilkins, *Medical engineering & physics*, **17**, 416 (1995).